



Physical immune escape: Weakened mechanical communication leads to escape of metastatic colorectal carcinoma cells from macrophages

Chen Yang^{a,b}, Xinrui Dong^{b,c}, Bingrui Sun^{b,c}, Ting Cao^d , Ruipei Xie^b, Yiyu Zhang^b , Ziyue Yang^{b,c}, Jing Huang^e, Ying Lu^b , Ming Li^b , Xiaochen Wang^{b,f,1}, Ye Xu^{a,1} , Fangfu Ye^{b,f,1} , and Qihui Fan^{b,1}

Edited by David Weitz, Harvard University, Cambridge, MA; received December 23, 2023; accepted April 29, 2024

The significance of biochemical cues in the tumor immune microenvironment in affecting cancer metastasis is well established, but the role of physical factors in the microenvironment remains largely unexplored. In this article, we investigated how the mechanical interaction between cancer cells and immune cells, mediated by extracellular matrix (ECM), influences immune escape of cancer cells. We focus on the mechanical regulation of macrophages' targeting ability on two distinct types of colorectal carcinoma (CRC) cells with different metastatic potentials. Our results show that macrophages can effectively target CRC cells with low metastatic potential, due to the strong contraction exhibited by the cancer cells on the ECM, and that cancer cells with high metastatic potential demonstrated weakened contractions on the ECM and can thus evade macrophage attack to achieve immune escape. Our findings regarding the intricate mechanical interactions between immune cells and cancer cells can serve as a crucial reference for further exploration of cancer immunotherapy strategies.

mechanical signals | immune escape | extracellular matrix

Cancer metastasis, a complex and daunting challenge, hinges on cancer cells' ability to evade immune cell attacks, breach the extracellular matrix (ECM), and migrate to other places to form secondary tumors (1). While the significance of the tumor immune microenvironment in affecting cancer cells' immune escape and metastasis is well established, research has primarily focused on biochemical cues, leaving the role of physical factors within microenvironment largely unexplored. In particular, how the mechanical interaction between cancer cells and immune cells mediated by ECM may influence cancer cells' immune escape is unclear.

Mechanical signals within the microenvironment are crucial for regulating biological processes and have recently obtained interest in immune activities (2–7). Among the immune cells, macrophages serve as a primary defense barrier, dynamically migrating to eliminate foreign substances and abnormal cells, such as cancer cells (8). Remarkably, Yang et al. discovered a fascinating physical mechanism complementary to the traditional chemotaxis, in which macrophages target breast cancer cells via ECM-transmitted paratensile signals (9). This mechanism involves mechanosensitive ion channel proteins, Ca^{2+} , and cytoskeletal proteins (10–13). However, the mechanoresponsiveness of macrophages to cancer cells with different metastatic potentials and the relation between this mechanoresponsiveness and the strategies employed by cancer cells to evade immune attacks from macrophages remain unclear.

To address these gaps in knowledge, we constructed an *in vitro* quasi-3D coculture system, in which a type I collagen hydrogel was used as ECM to simulate the *in vivo* microenvironment and investigated the response of macrophages to two distinct types of colorectal carcinoma (CRC) cells (SW480 and SW620), which possess different metastatic potentials. To evaluate these responses, we employed particle image velocimetry (PIV) to measure the ECM deformation induced by cancer cells' traction and used a micromanipulator-controlled microcapillary to mimic the traction forces exerted by the two different types of cancer cells on the ECM. Our results indicate that the CRC cells' traction forces can greatly influence macrophages' targeting efficiency and that weakened mechanical communication enables CRC cells with higher metastasis potential to evade macrophages and thus achieve enhanced immune escape.

Results and Discussion

SW480 and SW620 cells, derived from different colorectal cancer stages in the same patient, possess distinct tumorigenic properties. SW480 originates from the primary tumor, while SW620 is obtained from a lymph node metastasis during a second laparotomy (14). We aim to investigate ECM's influence on these two types of cells' immune escape, from a mechanobiological perspective.

Author affiliations: ^aSchool of Mechanical Engineering and Automation, Beihang University, Beijing 100191, China; ^bBeijing National Laboratory for Condensed Matter Physics, Institute of Physics, Chinese Academy of Sciences, Beijing 100190, China; ^cSchool of Physical Sciences, University of Chinese Academy of Sciences, Beijing 100049, China; ^dThe First Affiliated Hospital, School of Medicine, Zhejiang University, Hangzhou 310003, China; ^eDepartment of Immunology, School of Basic Medical Sciences, Peking University, Beijing 100191, China; and ^fOujiang Laboratory (Zhejiang Lab for Regenerative Medicine, Vision and Brain Health), Wenzhou Institute, University of Chinese Academy of Sciences, Wenzhou, Zhejiang 325000, China

Author contributions: J.H., F.Y., and Q.F. designed research; C.Y., X.D., B.S., X.W., Y.X., and Q.F. performed research; R.X., Y.L., and M.L. contributed new reagents/analytic tools; C.Y., X.D., T.C., Y.Z., Z.Y., and X.W. analyzed data; and C.Y., F.Y., and Q.F. wrote the paper.

The authors declare no competing interest.

Copyright © 2024 the Author(s). Published by PNAS. This open access article is distributed under [Creative Commons Attribution-NonCommercial-NoDerivatives License 4.0 \(CC BY-NC-ND\)](https://creativecommons.org/licenses/by-nc-nd/4.0/).

¹To whom correspondence may be addressed. Email: wangxiaocheda@ucas.ac.cn, ye.xu@buaa.edu.cn, fye@iphy.ac.cn, or fanqh@iphy.ac.cn.

This article contains supporting information online at <https://www.pnas.org/lookup/suppl/doi:10.1073/pnas.2322479121/-DCSupplemental>.

Published May 21, 2024.

To mimic the *in vivo* microenvironment, an *in vitro* quasi-3D coculture model was constructed, which integrated the collagen gel to provide mechanical support and signals. SW480 or SW620 cells were cocultured with macrophages (PMA-treated U937) on the top of 2 mg/mL collagen gel with a cell ratio of 1:25 (Fig. 1A). As shown in Fig. 1B, in the SW480 and macrophage coculture system, macrophages can precisely target to cancer cells SW480 from remote location and form adhesive cell aggregation (9); an obvious increase of attached macrophage ratio (with time) indicates that macrophages can continuously target to SW480 cells (Fig. 1C). In contrast, macrophages cocultured with SW620 cells, strikingly, do not show the tracing ability; the majority of the macrophages remain quiescent (Fig. 1B and C). This observation indicates that, compared with SW480 cells, SW620 cells in the coculture system have a larger chance to evade macrophages and thus achieve immune escape.

As a control test, cancer cells and macrophages were also cocultured on solid petri dish (without ECM), and the results show that the targeting ratio of macrophages to either SW620 or SW480 is less than 5%, indicating that ECM plays a critical role in inducing the aforementioned immune escape (Fig. 1C). Additionally, increasing the stiffness of the ECM from approximately 25 Pa to 100 Pa (SI Appendix) also results in fewer macrophages being attracted to the SW480 cells within 24 h (Fig. 1I). To answer this question, we dissect the investigation into two parts: We first investigate how these two types of cancer cells, respectively, may deform the ECM and change its microstructures and then investigate how macrophages may respond to given ECM deformations, which

are introduced by externally applied stress and used to mimic the deformations resulting from the two types of cancer cells.

To investigate the ECM deformation induced by the two types of cancer cells, SW480 and SW620 cells were, respectively, monocultured on top of 2 mg/mL collagen gel embedded with fluorescent microbeads markers, and the resulting deformations were analyzed with PIV. The results show that SW480 cells' traction force can generate a broad deformation range, which can reach to hundreds of micrometers in 12 h, whereas SW620 cells cannot produce detectable mechanical signals within 12 h (Fig. 1 E and F). To quantitatively characterize the deformations, we define two quantities: i) maximum displacement in the whole deformation field, u_{\max} , and ii) effective radius of deformation, r_e , with πr_e^2 equivalent to the magnitude of the area in which the ECM displacement is larger than 2 μm . The average values of u_{\max} and r_e for the measurements of 51 SW480 cells are given in Fig. 1 G and H, which in 12 h reaches to around 6 μm and 100 μm , respectively. It should be noted that almost all the u_{\max} values for SW620 cells are below 2 μm , a range that is challenging to differentiate from system noise. The microstructures of collagen fibers surrounding the cancer cells were imaged at 0 h and 6 h after the cell seeding, recorded using a confocal microscope (reflection mode). The corresponding results show that SW480 cells can remodel the collagen fibers and SW620 cannot (Fig. 1D). Notably, macrophages trivially remodel the surrounding ECM, hence avoiding self-induced mechanical interferences during mechanosensing of cancer cells (9).

We proceed to investigate macrophages' response to given ECM deformations. Physical tensile forces with controllable magnitude, applied by a customized micromanipulator-controlled negative

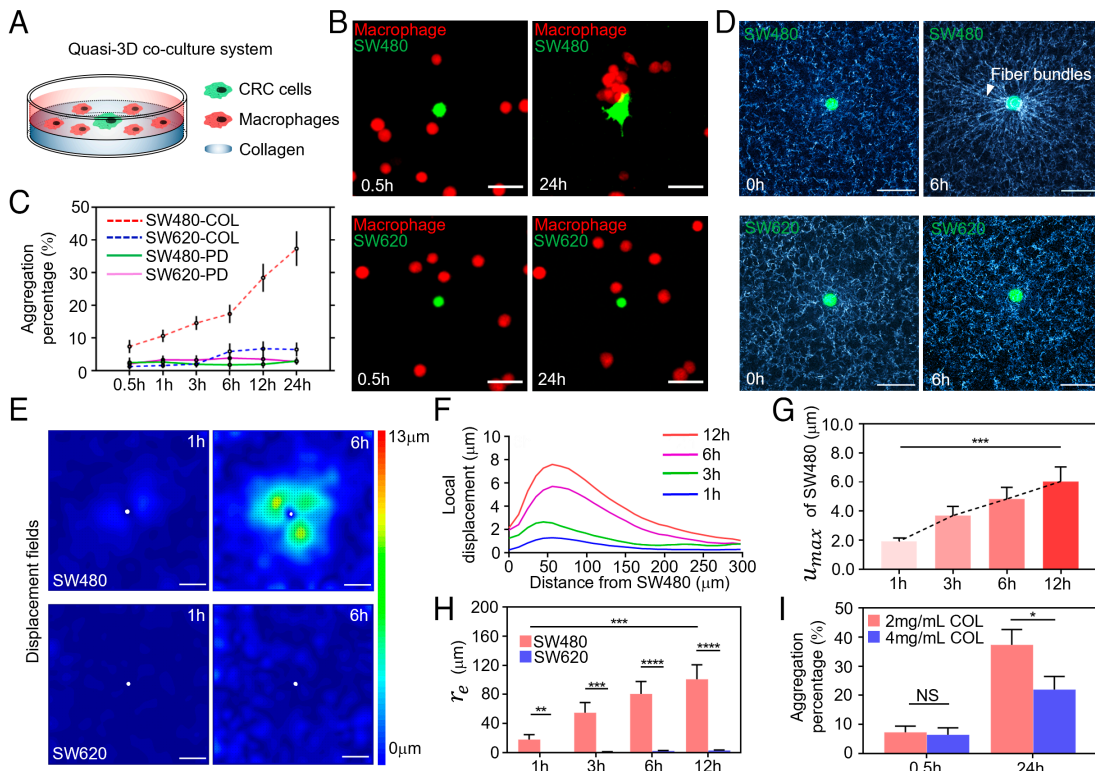


Fig. 1. (A) Schematic of *in vitro* quasi-3D coculture system of CRC cells and macrophages. (B) Time-lapse images of CRC cells (green) and macrophages (red) cocultured on top of 2 mg/mL collagen gel substrate. (Scale bars are 40 μm .) (C) Proportions of macrophages adhered to CRC cells cocultured on collagen (COL) substrate and solid petri dish (PD) substrate, within a 200 $\mu\text{m} \times 200 \mu\text{m}$ area centered on single cancer cells. Shown are means \pm SEM. (D) Cancer cells (green) and surrounding collagen matrix (white). The arrow indicates the collagen fiber bundles reconstructed by SW480 cells. (Scale bars are 50 μm .) (E) Representative magnitude maps of displacement fields induced by cancer cells. The color bar indicates the value of displacement. The white dots indicate the positions of cancer cells. (Scale bars are 100 μm .) (F) Local ECM displacement vs. distance from SW480 cells. (G) Maximum displacement, u_{\max} , of the ECM in a 200 $\mu\text{m} \times 200 \mu\text{m}$ area centered on SW480 after 1, 3, 6, and 12 h ($n = 51$). (H) Effective radius of deformation, r_e , induced by the traction force of SW480 ($n = 51$) and SW620 cells ($n = 54$) after 1, 3, 6, and 12 h. (I) Proportions of macrophages adhered to SW480 cells on 2 mg/mL and 4 mg/mL collagen substrates, respectively ($n = 38$).

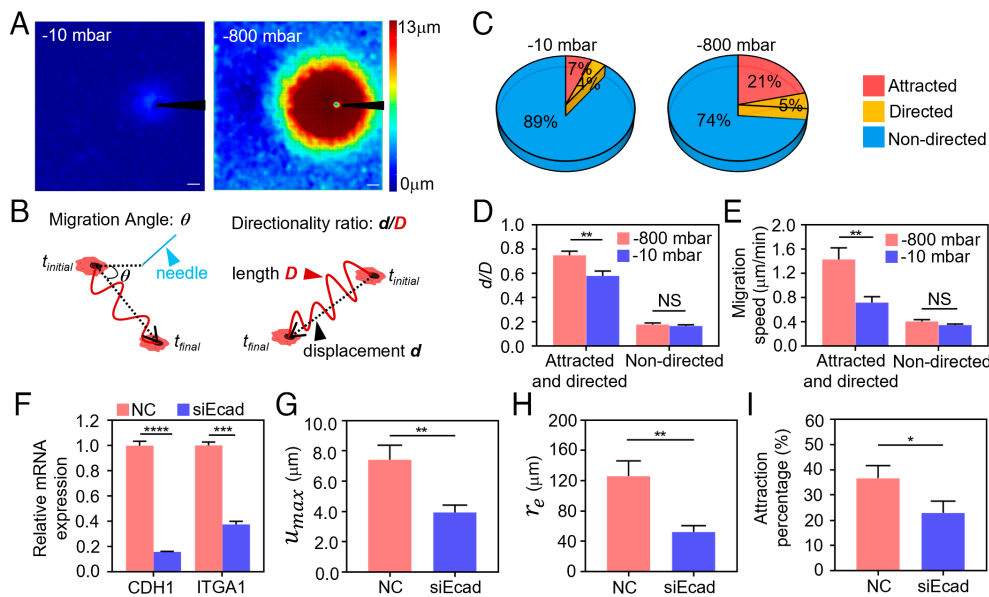


Fig. 2. (A) Magnitude maps of displacement fields induced by microcapillaries at -10 mbar and -800 mbar pressures, respectively. Scale bars are 100 μ m. (B) Definition of cell migration angle θ and directionality ratio d/D . (C) Ratio of macrophages in the attracted, directed, and non-directed categories. (D) Directionality ratio d/D and (E) migration speed of macrophages with different mechanoresponses in -800 mbar (red) and -10 mbar (blue) groups. (F) Relative mRNA expression of E-cadherin (CDH1) and $\alpha 1$ -integrin (ITGA1) in groups of NC (negative control, treated with scrambled siRNA) and siEcad (siRNA targeting E-cadherin). (G) u_{max} and (H) r_e of SW480 cells after 12 h in groups of NC ($n = 44$) and siEcad ($n = 46$) on 2 mg/mL collagen gel substrate. (I) Attraction percentages of macrophages toward SW480 cells after 12 h in groups of NC and siEcad.

pressure microcapillary system, are introduced to mimic the high and low contraction forces of cancer cells and the resulting ECM deformations (Fig. 2A). To characterize the response, we classify all trajectories of the cell migration subjected to externally applied forces into three categories (attracted, directed, and nondirected) according to the d/D (directionality ratio) and θ (migration angle) (Fig. 2B and *SI Appendix*) (9). The results show that 26% macrophages are responsive (i.e., either attracted or directed) for strong external stimuli (-800 mbar negative pressure applied on collagen via the microcapillary) while only 11% macrophages are responsive for weak external stimuli (-10 mbar negative pressure applied) (Fig. 2C). Moreover, the directionality ratio and the migration speed of macrophages also increase when the strength of the stimuli increases (Fig. 2 D and E).

In conclusion, the different ECM deformations resulting from SW480 and SW620 and the different responses of macrophages to different ECM deformations induced by externally applied forces, together, indicate that the tensile-force signaling transmitted through ECM plays an important role in determining macrophages' targeting efficiency and cancer cells' immune escape ability: cancer cells with low metastatic potential (SW480 cells) induce large ECM reconstruction and deformation, allowing macrophages to sense their emitted mechanical signals and target toward them, and highly metastatic cancer cells (SW620) in contrast can evade macrophages due to their weakened mechanical contraction on the ECM. To further verify the role of ECM-mediated force in the immune escape of cells with different metastatic abilities, we reduced the E-cadherin expression of SW480 cells to increase their metastatic ability, by using small interfering RNA (siRNA) (Fig. 2F and *SI Appendix*). The siRNA targeting E-cadherin SW480 (siEcad-SW480) exhibited weaker traction ability on ECM (Fig. 2 G and H), because the

expression of Integrin $\alpha 1\beta 1$, which is important for cell–collagen adhesion (15), in siEcad-SW480 cells was accordingly reduced (Fig. 2F), and the efficiency of macrophage targeting within the corresponding coculture system was also decreased (Fig. 2I). These results confirm that cancer cells with higher metastatic ability yield weaker forces and accordingly weaker attraction to macrophages. Our findings can provide valuable insights into the immune response of macrophages against cancer cells and serve as an important reference for future cancer immunotherapy strategies.

Materials and Methods

Detailed procedures are described in SI. Rat tail tendon type I collagen (Corning) solutions were prepared to construct the ECM in the quasi-3D system. For cell trajectory tracking experiments, 0.87- μ m-diameter fluorescent microbeads (Sphero) were premixed in the ECM as position markers. The E-cadherin expression was reduced by using specifically designed siRNA, and the changes of mRNA expression were measured by using qRT-PCR. To mimic the contractions of cancer cells, mechanical force loads were precisely applied to collagen substrate through glass microcapillaries (Sutter Instrument) controlled by programmed micromanipulator (Eppendorf, InjectMan) and a pressure controller (Elveflow, OB1 MK3).

Data, Materials, and Software Availability. All study data are included in the article and/or [supporting information](#).

ACKNOWLEDGMENTS. This work was supported by the National Key Research and Development Program of China (Grant Nos. 2022YFA1405002 and 2020YFA0908200), the National Natural Science Foundation of China (Grant Nos. 12325405, T2221001, 12074407, 12090054, 12072010, and 12304253), the Strategic Priority Research Program of Chinese Academy of Sciences (Grant No. XDB33000000), and the Youth Innovation Promotion Association of CAS (No. 2021007).

1. C. H. Stuelten, C. A. Parent, D. J. Montell, Cell motility in cancer invasion and metastasis: Insights from simple model organisms. *Nat. Rev. Cancer* **18**, 296–312 (2018).
2. R. Basu *et al.*, Cytotoxic T cells use mechanical force to potentiate target cell killing. *Cell* **165**, 100–110 (2016).
3. E. Natkanski *et al.*, B cells use mechanical energy to discriminate antigen affinities. *Science* **340**, 1587–1590 (2013).
4. A. G. Solis *et al.*, Mechanosensation of cyclical force by PIEZO1 is essential for innate immunity. *Nature* **573**, 69–74 (2019).
5. B. Aykut *et al.*, Targeting Piezo1 unleashes innate immunity against cancer and infectious disease. *Sci. Immunol.* **5**, eabb5168 (2020).
6. M. Huse, Mechanical forces in the immune system. *Nat. Rev. Immunol.* **17**, 679–690 (2017).
7. Q. Fan *et al.*, Dynamically re-organized collagen fiber bundles transmit mechanical signals and induce strongly correlated cell migration and self-organization. *Angew. Chem. Int. Ed. Engl.* **60**, 11858–11867 (2021).
8. I. Shihab *et al.*, Understanding the role of innate immune cells and identifying genes in breast cancer microenvironment. *Cancers* **12**, 2226 (2020).
9. C. Yang *et al.*, Dynamically reconstructed collagen fibers for transmitting mechanical signals to assist macrophages tracing breast cancer cells. *Adv. Funct. Mater.* **33**, 2211807 (2023).
10. M. L. Dustin, Integrins and their role in immune cell adhesion. *Cell* **177**, 499–501 (2019).
11. Y. C. Lin *et al.*, Force-induced conformational changes in PIEZO1. *Nature* **573**, 230–234 (2019).
12. C. Zhu, W. Chen, J. Lou, W. Rittase, K. Li, Mechanosensing through immunoreceptors. *Nat. Immunol.* **20**, 1269–1278 (2019).
13. Y. L. Han *et al.*, Cell contraction induces long-ranged stress stiffening in the extracellular matrix. *Proc. Natl. Acad. Sci. U.S.A.* **115**, 4075–4080 (2018).
14. E. S. Bergmann-Leitner, S. I. Abrams, Differential role of Fas/Fas ligand interactions in cytosis of primary and metastatic colon carcinoma cell lines by human antigen-specific CD8+ CTL. *J. Immunol.* **164**, 4941–4954 (2000).
15. J. Jokinen *et al.*, Integrin-mediated cell adhesion to type I collagen fibrils. *J. Biol. Chem.* **279**, 31956–31963 (2004).